HHS Public Access

Author manuscript

J Am Chem Soc. Author manuscript; available in PMC 2019 June 20.

Published in final edited form as:

J Am Chem Soc. 2018 June 20; 140(24): 7674–7680. doi:10.1021/jacs.8b03781.

A Fluorescent Metallacage-cored Supramolecular Polymer Gel Formed by Orthogonal Metal-Coordination and Host-Guest Interactions

Chenjie Lu[†,#], **Mingming Zhang**[*,‡,§,#], **Danting Tang**[†], **Xuzhou Yan**[§], **ZeYuan Zhang**[‡], **Zhixuan Zhou**[§], **Bo Song**[‖], **Heng Wang**[‖], **Xiaopeng Li**[‖], **Shouchun Yin**[*,†,§], **Hajar Sepehrpour**[§], and **Peter J. Stang**[*,§]

[†]College of Material, Chemistry and Chemical Engineering, Hangzhou Normal University, Hangzhou 310036, P. R. China

[‡]State Key Laboratory for Mechanical Behavior of Materials, Xi'an Jiaotong University, Xi'an 710049, P. R. China

[§]Department of Chemistry, University of Utah, 315 South 1400 East, Room 2020, Salt Lake City, Utah 84112, United States

[‖]Department of Chemistry, University of South Florida, 4202 East Fowler Ave, Tampa, Florida 33620, United States

Abstract

Herein, we report the preparation of a multi-functional metallacage-cored supramolecular gel by orthogonal metal-coordination and host-guest interactions. A tetragonal prismatic cage with four appended 21-crown-7 (21C7) moieties in its pillar parts was first prepared via the metal-coordination-driven self-assembly of *cis*-$Pt(PEt_3)_2(OTf)_2$, tetraphenylethene (TPE) based sodium benzoate ligands and linear dipyridyl ligands. Further addition of a bisammonium linker to the cage delivered a supramolecular polymer network via the host-guest interactions between the 21C7 moieties and ammonium salts, which formed a supramolecular gel at relatively higher concentrations. Due to the incorporation of a TPE derivative as the fluorophore, the gel shows emission properties. Multiple stimuli-responsiveness and good self-healing properties were also observed because of the dynamic metal-coordination and host-guest interactions used to stabilize the whole network structure. Moreover, the storage and loss moduli of the gel are 10-fold of the gel without the metallacage cores, indicating that the rigid metallacage plays a significant role in enhancing the stiffness of the gel. The studies described herein not only enrich the functionalization of fluorescent metallacages via elegant ligand design but also provide a way to prepare stimuli-responsive and self-healing supramolecular gels as robust and smart materials.

[*]**Corresponding Author:** mingming.zhang@xjtu.edu.cn, yinsc@hznu.edu.cn, stang@chem.utah.edu.

[#]C. L. and M. Z. contributed equally to this work.

Supporting Information

The supporting information is available free of charge via the Internet at http://pubs.acs.org.

Syntheses and characterization data (NMR, ESI-TOF-MS, Fluorescence Spectra), including Figures S1–S22.

The authors declare no competing financial interest.

Graphical Abstract

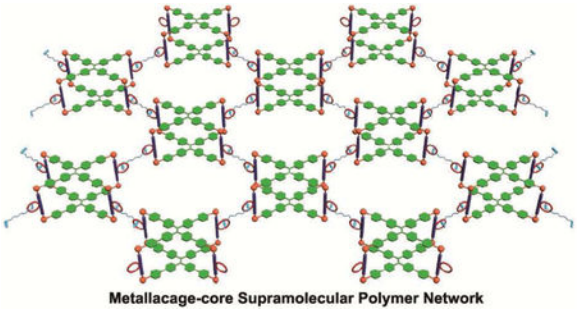

INTRODUCTION

Supramolecular gels,[1] as a remarkable class of soft materials linked by non-covalent interactions, have received much attention due to their wide applications in sensing and actuating,[2] catalysis and separation,[3] light-harvesting,[4] biomedical engineering,[5] etc. The dynamic and reversible nature of non-covalent interactions oftentimes benefits supramolecular gels stimuli-responsiveness and self-healing properties.[6] Although various non-covalent interactions including metal-coordination and host-guest interactions have been widely used to prepare supramolecular gels, the formation of supramolecular gels via multiple orthogonal interactions[7] not only offers more functionalities such as optical and electric properties but also gives a pathway for hierarchical self-assembly to mimic biological systems. For example, we reported a responsive supramolecular polymer gel via the orthogonal metal-coordination and crown ether-based host-guest interactions, showing the advantages of orthogonal self-assembly in the preparation of stimuli-responsive materials.[8] Through the introduction of extra hydrogen bonding interactions to this system, the functionalization of supramolecular gels was engineered.[9] Metallacycle-core supramolecular polymers with tunable fluorescence were also prepared via orthogonal self-assembly by the incorporation of fluorophores in this system.[10]

Metallacages (or metal-organic cages) represent an important class of structures in metal-coordination-driven chemistry not only due to their appealing structures but also because they can work as “molecular flasks” for chemical reactions, benefiting guest molecules with reactivities different from those in bulk solutions.[11] Although vast of metallacages have been prepared during last two decades, fluorescent metallacage-core supramolecular gels have never been reported yet.[12] The introduction of fluorescent metallacages not only bring high branch functionalities[12c] but also benefits the gels emission properties, which may serve as a platform for light-harvesting applications. Through the introduction of tetraphenylethene (TPE) derivatives which show aggregation induced emission (AIE)[13]properties, our group has prepared a series of fluorescent metallacages that display good emissions both in the aggregated state and in dilute solutions.[14] Encouraged by the progress we have made on emissive cages and supramolecular polymers formed by orthogonal self-assembly, we prepared a fluorescent metallacage-cored supramolecular gel by the further introduction of crown ether-based host-guest interactions to one of these emissive cages. A crown ether-decorated tetragonal prismatic cage was first prepared and well characterized. Based on the

host-guest interactions between the appendant crown ethers and secondary ammonium salts,[15] a bisammonium linker was added to cross-link the cage to give a supramolecular polymer network (SPN), which would transfer to a supramolecular gel at high concentrations. The gel possesses several characteristics: 1) It is emissive due to the incorporated metallacages with AIE properties because both the formation of gels and the highly emissive properties of AIE fluorophores call for high concentrations or aggregations; 2) It exhibits reversible gel-sol transitions induced by heat and potassium ions due to the dynamic and reversible nature of metal-coordination and host-guest interactions; 3) It shows enhanced stiffness compared with a model gel without metallacage as the core parts due to the rigidity of the metallacages and the high branch functionality when the metallacages are used as the junctions; 4) It exhibits excellent self-healing properties, which can not only be observed directly from their optical photos, but also revealed by rheological study. All these characteristics show the unmatched advantages of the introduction of AIE-active metallacages into supramolecular gels, in which multiple functions including fluorescence, stimuli-responsiveness, self-healing as well as improved stiffness can be realized simultaneously in a single supramolecular gel system.

RESULTS AND DISCUSSION

Preparation and Characterizations of Metallacage

Based on the self-assembly of TPE-based sodium benzoate **1**, *cis*-$Pt(PEt_3)_2(OTf)_2$ **2** and a 21-crown-7 (21C7) appendant dipyridyl ligand **3**, cage **4** was prepared in 91% isolated yield according to our previous reported method[14e] (Scheme 1a). The cage was characterized by multiple NMR (^1H NMR and $^{31}P\{^1H\}$ NMR) and ESI-TOF-MS (Figure 1). The $^{31}P\{^1H\}$ NMR spectrum (Figure 1b) of cage **4** exhibits two doublets of equal intensity with concomitant ^{195}Pt satellites at 7.69 and 2.58 ppm, indicating the formation of a discrete, charge-separated metallacage.[14] In the ^1H NMR spectra of **4**, downfield shifts were observed for α-pyridyl protons H_e (from 8.70 ppm to 8.84 ppm) and β-pyridyl protons H_f (from 7.86 ppm to 8.02 ppm) as compared to the free dipyridyl ligand **3** (Figure 1, spectra e and f), due to the formation of Pt(II)←pyridine coordination bonds. The aromatic protons H_g, H_h and H_i and ethoxy protons H_α and H_β shifted upfield, which is consistent with previous reports.[10] ESI-TOF-MS provides the evidence for the stoichiometry of cage **4**. Peaks at m/z = 938.84, 1097.70, 1301.50, 1591.63, 2027.36 were observed and isotopically well-resolved (Figures 1c and S11), corresponding to $[M - 8OTf]^{8+}$, $[M - 7OTf]^{7+}$, $[M - 6OTf]^{6+}$, $[M - 5OTf]^{5+}$ and $[M - 4OTf]^{4+}$, respectively (where M represents the intact assembly).

The fluorescence spectra of cage **4** was then recorded in acetone/hexane mixtures (Figure S18) to investigate the AIE properties of **4**. The addition of hexane into the acetone solutions decreases the solubility of cage **4** and thereby leads to the formation of aggregates. Cage **4** shows a moderate emission centered at 497 nm in pure acetone. Upon the gradual increase of hexane content, the fluorescent intensities increased and reached a maximum value at the hexane fraction of 95%, indicating that cage **4** is AIE-active, consistent with our previous reports on emissive platinum(II) cages.[14] This property is crucial for the preparation of emissive gels because both the good emission of AIE-active fluorophores and the formation of gels require highly concentrated states.

Self-assembly of Supramolecular Gel

^{1}H NMR established the host-guest complexation between cage **4** and bisammonium linker **5**. Obvious chemical shift changes were observed by the comparison of the ^{1}H NMR spectra of cage **4**, linker **5** and their mixture (Figure 2). The methylene protons H_1, benzyl protons H_2, and aromatic protons H_3 and H_4 of linker **5** shifted upfield, whereas the protons H_α and H_β shifted downfield. No obvious chemical shift changes were observed for the aromatic protons $H_{a\text{-}i}$ of cage **4**. These results indicated the existence of 21C7/ammonium salt complexation in the SPN **6**,[15] which provides the intramolecular interactions for the formation of supramolecular gels at high concentrations. Based on the concentration-dependent ^{1}H NMR (Figure S20) measurements, the peaks for the signals of all the protons became more and more broad as the concentration increased, suggesting the gradual formation of SPNs.[16]

Two-dimensional diffusion-ordered NMR spectrascopy (DOSY) (Figure 3a) and dynamic light scattering (DLS) measurments (Figure 3b) were also carried out to determine the size of the aggregates fromed by cage **4** and cross-linker **5** in solution. As the concentration of 21C7/ammonium salt increased from 1.0 mM to 50 mM, the measured weight average diffusion coefficient decreased from 2.5×10^{-9} m^2 s^{-1} to 2.4×10^{-10} m^2 s^{-1} ($D_{1.0\text{mM}}$/$D_{50\text{mM}}$ = 10.4) and the average hydrodynamic diameter (D_h) increased from 160 nm to 470 nm, indicating the formation of high molecular weight SPNs. Scanning electronic microscopy (SEM) revealed an interconnected porous structure with entangled nanofibers for SPN (Figure 3c), indicating that cross-linked networks were formed.

Then the gelation process of the SPN was studied. Cage **4** (80.0 mM) and bis-ammonium linker **5** (160 mM) were dissolved in acetone, separately. When the two solutions were mixed, a metallacage-cored supramolecular gel formed immediately. The final concentration of the gel was 160 mM in crown ether/ammonium salt concentration.[17] The gel shows thermo- and potassium ion-induced gel-sol transitions, which can be overserved visually (Figure 4). This is because both the heating and the addition of KPF_6 weaken the host-guest interactions between 21C7 and ammonium salts, leading to the destruction of the SPNs and inducing the sol formation. The gel recovers upon cooling or the further addition of 18-crown-6 (18C6). This gel-sol process may also be monitored by the changes of fluorescence intensity (Figures 3d and S21) because of the AIE-active metallacage incorporated in this system. The fluorescence of the gel decreases upon heating or by the addition of KPF_6 and returns its original state upon cooling or by the succeed addition of 18C6. The transition from gel to sol decreases the aggregation of the metallacages, responsible for the observed decreased fluorescence. When the reverse process happens, the fluorescence recovers. The reversible conversions were also evidenced by ^{1}H NMR experiments (Figures S22).

The quantum yields of metallacage **4** in acetone and gel **6** were measured to be 2.65% and 4.55%, respectively. The formation of supramolecular networks leads to the aggregation of metallacage **4**, which will further restrict the free rotation of the phenyl groups of **1**, responsible for the increased quantum yields. The quantum yields of **4** in the solid state and xerogel **6** were 6.12% and 5.71%, respectively. In the solid state, the molecular packing density in xerogel **6** is lower than that in **4** due to the addition of flexible linkers. Because

molecular packing plays a more important role in the solid-state emission of TPE derivatives,[13] the quantum yield of xerogel **6** is lower than that of metallacage **4**.

Self-healing and Rheological Study

The metallacage-cored gel exhibits macroscopically self-healing properties which could be visually observed. It can be seen from Figure 5 that the crack on the gel totally disappeared after 4.0 min. The dynamic and reversible metal-coordination and host-guest interactions are responsible for the self-healing process. When the gel is broken, the non-covalent interactions on the edge of the crack are also destroyed. However, due to their dynamic and reversible nature, they would recover in a short time to trigger the healing.

To gain further insights on the influence of the metallacages as junctions in the gel, a model gel **8** was prepared by the self-assembly of a TPE-cored crown ether **7** and bisammonium salt **5** (Scheme 2) at the same concentration as that of gel **6** (160 mM 21C7/ammonium salt concentration). Rheological experiments (Figure 6) were carried out to characterize the two gels. For gels **6** and **8**, the storage modulus (G') is larger than loss modulus (G'') and G' is independent of the angular frequency ω (Figure 6, spectra a and d), indicating the formation of organogels. It is worth mentioning that the G' of gel **6** is ca. 10-fold of that of gel **8**, indicating that gel **6** is much stiffer than gel **8**. This is attributed to the rigidity of the metallacages and higher branch functionalities when metallacages are used as the junctions.[12c] Further improvement of the stiffness of the gels could be achieved by increasing the active cross-links, such as increasing the crown ether units per cage or using tetra-ammonium salts as the cross-linker.

The self-healing properties of gels **6** and **8** were also studied by rheological tests. The gels were subjected to strain sweep tests (Figure 6, spectra b and e) to get the broken strains of the two gels. Then the two gels were investigated under large (300%) and small (0.1%) strains, respectively (Figure 6, spectra c and f). The G' is smaller than G'' under 300% strain, indicating that the gels were broken. For gel **6**, when the strain was released to 0.1%, both G' and G'' returned to their original values, and this process was repeated for 4 times without any loss of the modulus. While for gel **8**, G' and G'' only recovered to 85% of their original values in each cycle. These observations indicate that gel **6** shows better self-healing properties than gel **8**. The involvement of rigid metallacages as the junctions not only enhances the stiffness of the gels, but also improves the self-healing properties.

CONCLUSION

In summary, we have prepared a metallacage-cored supramolecular gel by the orthogonal self-assembly of metal-coordination and host-guest interactions between 21C7 and ammonium salts. A combination of ^{1}H NMR, DOSY, DLS, fluorescence spectroscopy, SEM and rheology was used to study the network structures and properties of the gel. The introduction of metallacages as the junctions not only benefits the supramolecular gel emission properties, but also gives enhanced stiffness and improved self-healing properties for the gel. Thermo- and cation-responsiveness, derived from the dynamic nature of non-covalent interactions in this system, is well preserved. The introduction of AIE-active fluorophores into gel systems offers a good method to prepare luminescent gels to avoid the

fluorescence quenching caused by the highly aggregated state of molecules in gels. Considering most supramolecular gels are too “soft” for practical applications, strengthening the gels by the incorporation of metallacage structures as junctions seems commendable because it also improves the self-healing properties of the gels while keeping their stimuli-responsiveness. This study provides an efficient approach to develop multiple-functional supramolecular gels by orthogonal self-assembly and opens a new avenue on the construction of dynamic yet robust supramolecular materials.

EXPERIMENTAL SECTION

Full experimental details are provided in the Supporting Information. The most important information is summarized below.

Materials and Methods.

All reagents were commercially available and used as supplied without further purification. Deuterated solvents were purchased from Cambridge Isotope Laboratory (Andover, MA). **1**[18] and **2**[19] were prepared according to the literature procedures. NMR spectra were recorded on a Varian Unity 300 MHz or 400 MHz spectrometer. ^{1}H and ^{13}C NMR chemical shifts are reported relative to residual solvent signals, and ^{31}P{^{1}H} NMR chemical shifts are referenced to an external unlocked sample of 85% H_3PO_4 (δ = 0.0). Mass spectra were recorded on a Micromass Quattro II triple-quadrupole mass spectrometer using electrospray ionization with a MassLynx operating system. The melting points were collected on a SHPSIC WRS-2 automatic melting point apparatus. The UV-vis experiments were conducted on a Hitachi U-4100 absorption spectrophotometer. The fluorescent experiments were conducted on a Hitachi F-7000 fluorescence spectrophotometer. Scanning electron microscopy (SEM) was performed on a FEI Quanta 600 FEG. Dynamic light scattering experiments were performed using a Malvern ZS90 instrument with a He-Ne laser (633 nm) and 90° collecting optics. The data were analyzed using the Malvern Dispersion Technology Software 5.10. Rheological data were obtained by using a ARES-G2 rheometer (Waters) with plate-plate geometry (diameter of 25 mm, gap is 200 μm). Oscillatory frequency sweep experiments were performed from 0.1 rad/s to 100 rad/s with a strain in the linear region at 20 °C. The scanning frequency of self-healing experiments were performed was 10 rad/s^{-1} at 20°C.

Self-assembly of ***4*****.** **1** (2.25 mg, 2.50 μmol), **2** (7.30 mg, 10.0 μmol) and **3** (3.05 mg, 5.00 μmol) were mixed in a 1:4:2 molar ratio and dissolved in acetone/water (1.0 mL, 4:1, v/v). The whole reaction mixture was heated at 50 °C for 12 h and then cooled to room temperature. The solvent was removed by nitrogen flow. The residue was dissolved in acetone (1.0 mL), filtered and the filtrate was poured into ethyl ether (10.0 mL) to give a precipitate, which was collected by centrifugation to give cage **4** (9.90 mg, 91%) as a pale-yellow powder. ^{1}H NMR (400 MHz, CD_3COCD_3, 295K): 8.98 (d, J = 6.1 Hz, 16H), 8.86 (d, J = 8.8 Hz, 8H), 8.48 (s, 8H), 8.04 (d, J = 6.1 Hz, 16H), 7.99 (d, J = 8.8 Hz, 8H), 7.64 (d, J = 8.2 Hz, 16H), 7.44 (d, J = 8.2 Hz, 16H), 7.35 (d, J = 8.2 Hz, 16H), 7.05 (d, J = 8.2 Hz, 16H), 4.25–4.32 (m, 16H), 3.86–3.91 (m, 16H), 3.78–3.83 (m, 16H), 3.71–3.75 (m, 16H), 3.60–3.66 (m, 32H). ^{31}P{^{1}H} NMR (121.4 MHz, CD_3COCD_3, 295 K): 7.69 ppm (d, $^{2}J_{P\text{-}P}$ = 20.6

Hz, ^{195}Pt satellites, $^{1}J_{\text{pt-P}}$ = 3350 Hz), 2.58 ppm (d, $^{2}J_{\text{P-P}}$ = 20.6 Hz, ^{195}Pt satellites, $^{1}J_{\text{pt-P}}$ = 3350 Hz). ESI-TOF-MS: *m/z* 938.84 [**4** – 8OTf]$^{8+}$, 1097.70 [**4** – 7OTf]$^{7+}$, 1301.50 [**4** – 6OTf]$^{6+}$, 1591.63 [**4** – 5OTf]$^{5+}$, 2027.36 [**4** – 4OTf]$^{4+}$.

*Preparation of gel **6***. Cage **4** (139 mg, 16.0 μmol) and bisammonium linker **5** (23.7 mg, 32.0 μmol) was dissolved in acetone (0.2 mL) in two separate vials. Then the solution of **5** was added to that of **4** to form a gel immediately, which was used for the fluorescence and rheological tests. The final concentration of the gel is 160.0 mM in crown ether/ammonium salt concentration.

*Preparation ofgel **8***. Compounds **7** (30.8 mg, 16.0 μmol) was dissolved in chloroform (0.2 mL) and bisammonium linker **5** (23.7 mg, 32.0 μmol) was dissolved in acetonitrile (0.2 mL) in two separate vials. Then the solution of **5** was added to that of **7** to form a gel. The solvent of the gel was removed to form a xerogel and then acetone (0.4 mL) was added to form an organogel in acetone. The final concentration of the gel is also 160.0 mM in crown ether/ ammonium salt concentration.

Supplementary Material

Refer to Web version on PubMed Central for supplementary material.

ACKNOWLEDGMENTS

S.Y. thanks the National Natural Science Foundation of China (21574034) and Zhejiang Provincial Natural Science Foundation of China (LY16B040006) for financial support. P.J.S. thanks National Institutes of Health (Grant R01 CA215157) for financial support. M.Z. is thankful for start-up funds from Xi'an Jiaotong University and the National Thousand Young Talents Program. X.L. thanks the National Science Foundation (CHE-1506722) and PREM Center of Texas State University (DMR-1205670) for financial support.

REFERENCES

(1). (a)Sangeetha N; Maitra U Chem. Soc. Rev 2005, 34, 821. [PubMed: 16172672] (b)Steed JW Chem. Commun 2011, 47, 1379.(c)Sun JY; Zhao X; Illeperuma WR; Chaudhuri O; Oh KH; Mooney DJ; Vlassak JJ; Suo Z Nature 2012, 489, 133. [PubMed: 22955625] (d)Yu G; Yan X; Han C; Huang F Chem. Soc. Rev 2013, 42, 6697. [PubMed: 23744396] (e)Voorhaar L; Hoogenboom R Chem. Soc. Rev 2016, 45, 4013. [PubMed: 27206244] (f)Zhang YS; Khademhosseini A Science 2017, 356, eaaf3627. [PubMed: 28473537] (f)Draper ER; Adams DJ Chem 2017, 3, 390.

(2). (a)Piepenbrock M-OM; Lloyd GO; Clarke N; Steed JW Chem. Rev 2010, 110, 1960. [PubMed: 20028020] (b)Veits GK; Carter KK; Cox SJ; McNeil AJ J. Am. Chem. Soc 2016, 138, 12228. [PubMed: 27598826] (c)Goujon A; Mariani G; Lang T; Moulin E; Rawiso M; Buhler E; Giuseppone NJ Am. Chem. Soc 2017, 139, 4923.(d)Wang H; Ji X; Li Z; Huang F Adv. Mater 2017, 29, 1606117(e)Ji X; Wu RT; Long L; Ke XS; Guo C; Ghang YJ; Lynch VM; Huang F; Sessler JL Adv. Mater 2018, 30, 1705480.(f)Zhang X; Wang J; Jin H; Wang S; Song WJ Am. Chem. Soc 2018, 140, 3186.

(3). (a)Trausel F; Versluis F; Maity C; Poolman JM; Lovrak M; van Esch JH; Eelkema R Acc. Chem. Res 2016, 49, 1440. [PubMed: 27314682] (b)Okesola BO; Smith DK Chem. Soc. Rev 2016, 45, 4226. [PubMed: 27241027] (c)Ji X; Wu RT; Long L; Guo C; Khashab NM; Huang F; Sessler JL J. Am. Chem. Soc 2018, 140, 2777. [PubMed: 29437394] (d)Zhang Y; Chan PPY; Herr AE Angew. Chem., Int. Ed 2018, 57, 2357.(e)Wang X; Wei C; Su JH; He B; Wen GB; Lin YW; Zhang Y Angew. Chem., Int. Ed 2018, 57, 3504.

(4). (a)Ajayaghosh A; Praveen VK; Vijayakumar C Chem. Soc. Rev 2008, 37, 109. [PubMed: 18197337] (b)Babu SS; Praveen VK; Ajayaghosh A Chem. Rev 2014, 114, 1973. [PubMed: 24400783] (c)Duan P; Yanai N; Nagatomi H; Kimizuka NJ Am. Chem. Soc 2015, 137, 1887. (d)Felip-León C; Díaz-Oltra S; Galindo F; Miravet JF Chem. Mater 2016, 28, 7964.(e)Gorai T; Maitra U Angew. Chem., Int. Ed 2017, 56, 10730.

(5). (a)Moon HJ; Ko du Y; Park MH; Joo MK; Jeong B Chem. Soc. Rev 2012, 41, 4860. [PubMed: 22688789] (b)Saxena S; Hansen CE; Lyon LA Acc. Chem. Res 2014, 47, 2426. [PubMed: 24873478] (c)Zhang SY; Bellinger AM; Glettig DL; Barman R; Lee YAL; Zhu JH; Cleveland C; Montgomery VA; Gu L; Nash LD; Maitland DJ; Langer R; Traverso G Nat. Mater 2015, 14, 1065. [PubMed: 26213897] (d)Shigemitsu H; Hamachi I Acc. Chem. Res 2017, 50, 740. [PubMed: 28252940] (e)Cooke ME; Jones SW; Ter Horst B; Moiemen N; Snow M; Chouhan G; Hill LJ; Esmaeli M; Moakes RJA; Holton J; Nandra R; Williams RL; Smith AM; Grover LM Adv. Mater 2018, 30, 1705013.

(6). (a)Wang Q; Mynar JL; Yoshida M; Lee E; Lee M; Okuro K; Kinbara K; Aida T Nature 2010, 463, 339. [PubMed: 20090750] (b)Nakahata M; Takashima Y; Yamaguchi H; Harada A Nat. Commun 2011, 2, 511. [PubMed: 22027591] (c)Zhang M; Xu D; Yan X; Chen J; Dong S; Zheng B; Huang F Angew. Chem., Int. Ed 2012, 51, 7011.(d)Chen H; Ma X; Wu S; Tian H Angew. Chem., Int. Ed 2014, 53, 14149.(e)Zheng W; Chen LJ; Yang G; Sun B; Wang X; Jiang B; Yin GQ; Zhang L; Li X; Liu M; Chen G; Yang HB J. Am. Chem. Soc 2016, 138, 4927. [PubMed: 27011050] (f)Zheng W; Yang G; Shao N; Chen LJ; Ou B; Jiang ST; Chen G; Yang HB J. Am. Chem. Soc 2017, 139, 13811. [PubMed: 28885839]

(7). (a)Li S-L; Xiao T; Lin C; Wang L Chem. Soc. Rev 2012, 41, 5950. [PubMed: 22773054] (b)Hu X-Y; Xiao T; Lin C; Huang F; Wang L Acc. Chem. Res 2014, 47, 2041. [PubMed: 24873508] (c)Wei P; Yan X; Huang F Chem. Soc. Rev 2015, 44, 815. [PubMed: 25423355]

(8). Yan X; Cook TR; Pollock JB; Wei P; Zhang Y; Yu Y; Huang F; Stang PJ J. Am. Chem. Soc 2014, 136, 4460. [PubMed: 24621148]

(9). Zhou Z; Yan X; Cook TR; Saha ML; Stang PJ J. Am. Chem. Soc 2016, 138, 806. [PubMed: 26761393]

(10). Zhang M; Yin S; Zhang J; Zhou Z; Saha ML; Lu C; Stang PJ Proc. Natl. Acad. Sci. USA 2017, 114, 3044. [PubMed: 28265080]

(11). (a)Inokuma Y; Kawano M; Fujita M Nat. Chem 2011, 3, 349. [PubMed: 21505492] (b)Brown CJ; Toste FD; Bergman RG; Raymond KN Chem. Rev 2015, 115, 3012. [PubMed: 25898212]

(12). (a)Foster JA; Parker RM; Belenguer AM; Kishi N; Sutton S; Abell C; Nitschke JR J. Am. Chem. Soc 2015, 137, 9722. [PubMed: 26153733] (b)Zhukhovitskiy AV; Zhong M; Keeler EG; Michaelis VK; Sun JE; Hore MJ; Pochan DJ; Griffin RG; Willard AP; Johnson JA Nat. Chem 2016, 8, 33. [PubMed: 26673262] (c)Uchida J; Yoshio M; Sato S; Yokoyama H; Fujita M; Kato T Angew. Chem., Int. Ed 2017, 56, 14085.

(13). (a)Zhao Z; Lam JWY; Tang BZ J. Mater. Chem 2012, 22, 23726.(b)Mei J; Hong Y; Lam JWY; Qin A; Tang Y; Tang BZ Adv. Mater 2014, 26, 5429. [PubMed: 24975272] (c)Mei J; Leung NL; Kwok RT; Lam JW; Tang BZ Chem. Rev 2015, 15, 11718.

(14). (a)Yan X; Cook TR; Wang P; Huang F; Stang PJ Nat. Chem 2015, 7, 342. [PubMed: 25803473] (b)Yan X; Wang M; Cook TR; Zhang M; Saha ML; Zhou Z; Li X; Huang F; Stang PJ J. Am. Chem. Soc 2016, 138, 4580. [PubMed: 26982213] (c)Yu G; Cook TR; Li Y; Yan X; Wu D; Shao L; Shen J; Tang G; Huang F; Chen X; Stang PJ Proc. Natl. Acad. Sci. USA 2016, 113, 13720. [PubMed: 27856738] (d)Saha ML; Yan X; Stang PJ Acc. Chem. Res 2016, 49, 2527. [PubMed: 27736060] (e)Zhang M; Saha ML; Wang M; Zhou Z; Song B; Lu C; Yan X; Li X; Huang F; Yin S; Stang PJ J. Am. Chem. Soc 2017, 139, 5067.

(15). (a)Zhang C; Li S; Zhang J; Zhu K; Li N; Huang F Org. Lett 2007, 9, 5553. [PubMed: 18047364] (b)Yan X; Xu D; Chi X; Chen J; Dong S; Ding X; Yu Y; Huang F Adv. Mater 2012, 24, 362. [PubMed: 22161963]

(16). (a)De Greef TFA; Smulders MMJ; Wolffs M; Schenning APHJ; Sijbesma RP; Meijer EW Chem. Rev 2009, 109, 5687. [PubMed: 19769364] (b)Yang L; Tan X; Wang Z; Zhang X Chem. Rev 2015, 115, 7196. [PubMed: 25768045]

(17). The very high concentration for the gel 6 to be formed might because the length of the linker 5 is relatively short, which will give low viscosity for the supramolecular polymer and ask for high concertation for the gelation.

(18). Zhang Q; Su J; Feng D; Wei Z; Zou X; Zhou HC J. Am. Chem. Soc 2015, 137, 10064. [PubMed: 26214704]

(19). Stang PJ; Cao DH; Saito S; Arif AM J. Am. Chem. Soc 1995, 117, 6273.

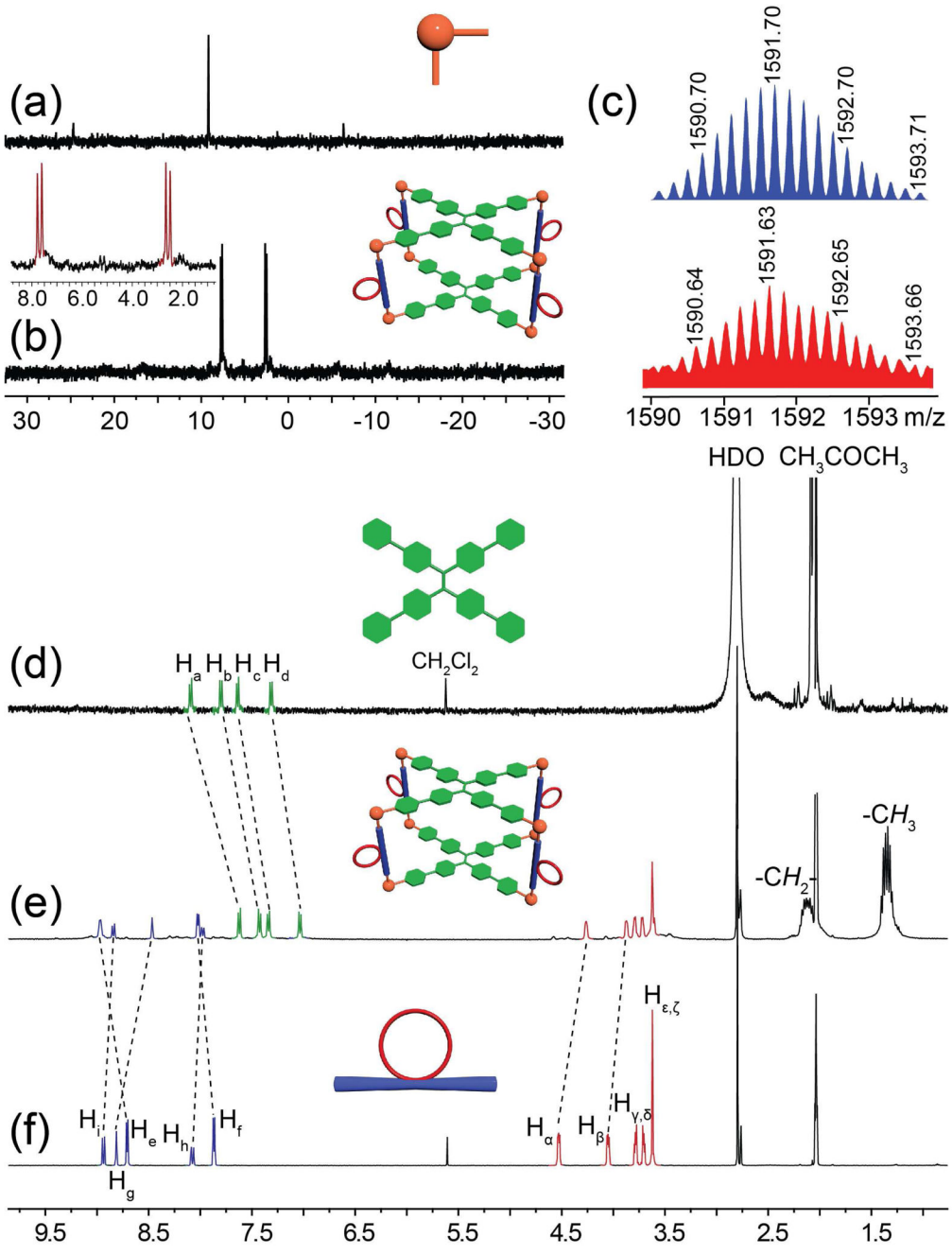

Figure 1.

^{31}P {^{1}H} NMR spectra (121.4 MHz, CD_3COCD_3, 295 K) of (a) **2** and (b) **4**. (c) Experimental (red) and calculated (blue) ESI-TOF-MS spectra of metallacage **4**: [**4** – 5OTf]$^{5+}$. Partial ^{1}H NMR spectra (400 MHz, CD_3COCD_3, 295 K) of (d) TPE derivative **1**, (e) metallacage **4** and (f) dipyridyl ligand **3**.

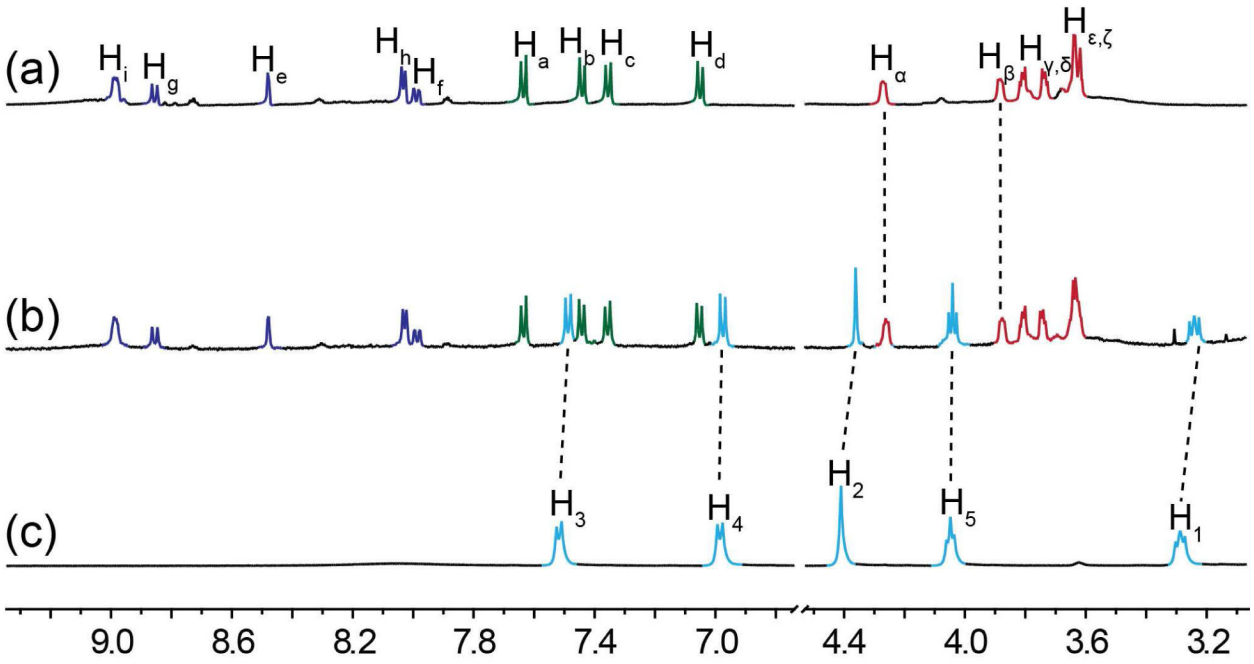

Figure 2.

Partial ^{1}H NMR spectra (400 MHz, CD_3COCD_3, 295 K) of (a) metallacage **4**, (b) a mixture of metallacage **4** and bisammonium salt **5** (1.00 mM 21C7/ammonium salt moieties) and (c) bisammonium salt **5**.

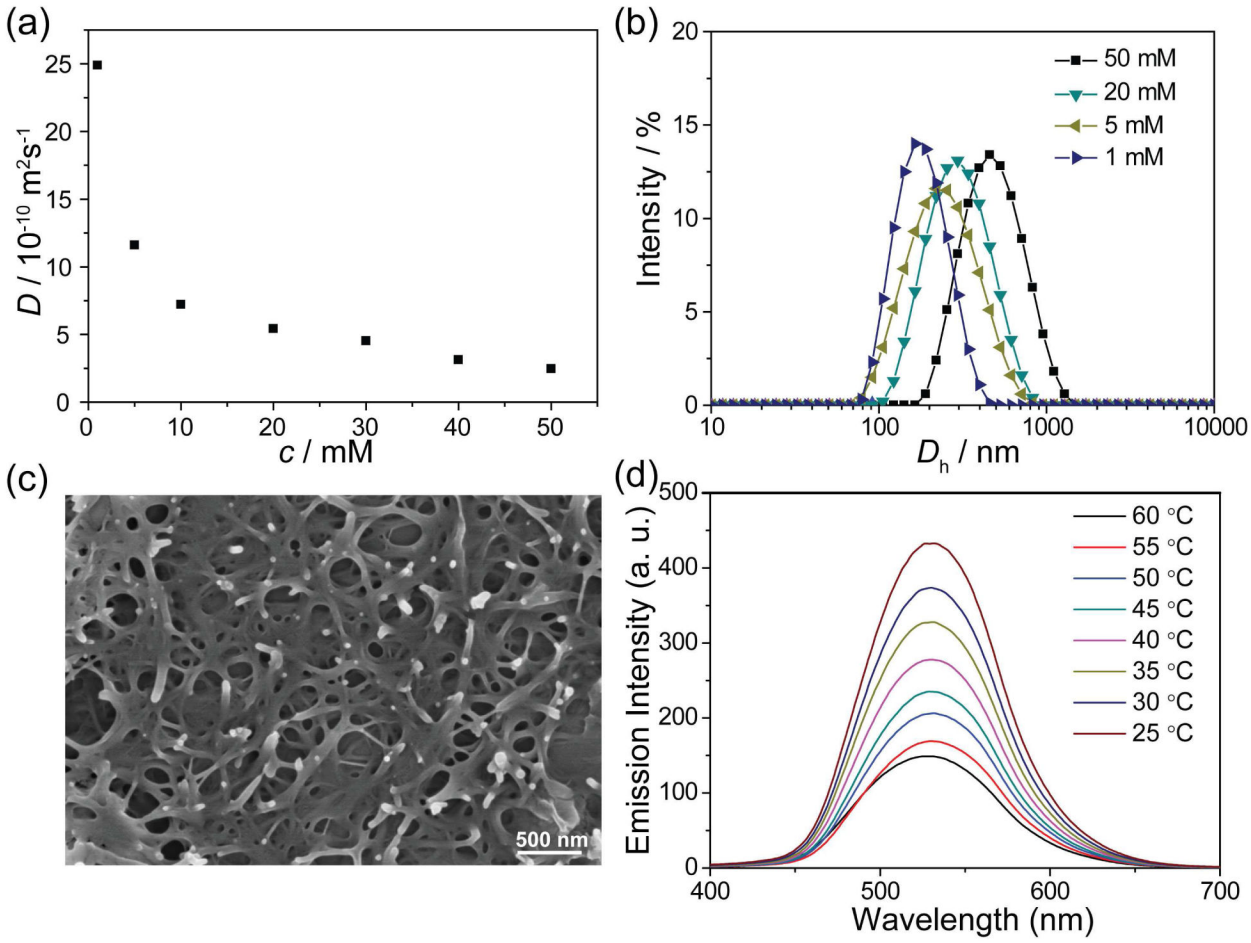

Figure 3.

(a) Concentration dependence of diffusion coefficient D (CD_3COCD_3, 295 K, 400 MHz) of SPN. (b) Size distributions of SPN at different concentrations in acetone. (c) SEM image of the SPN prepared by a freeze-drying method. (d) Temperature dependent fluorescence spectra of SPN (160 mM in acetone). Here the concentration of crown ether units is used as the concentration.

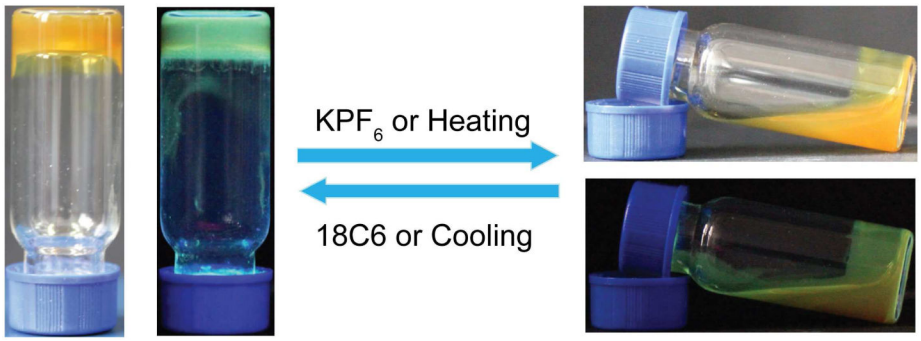

Figure 4.
Optical and fluorescence photographs of the reversible gel–sol transition of SPN.

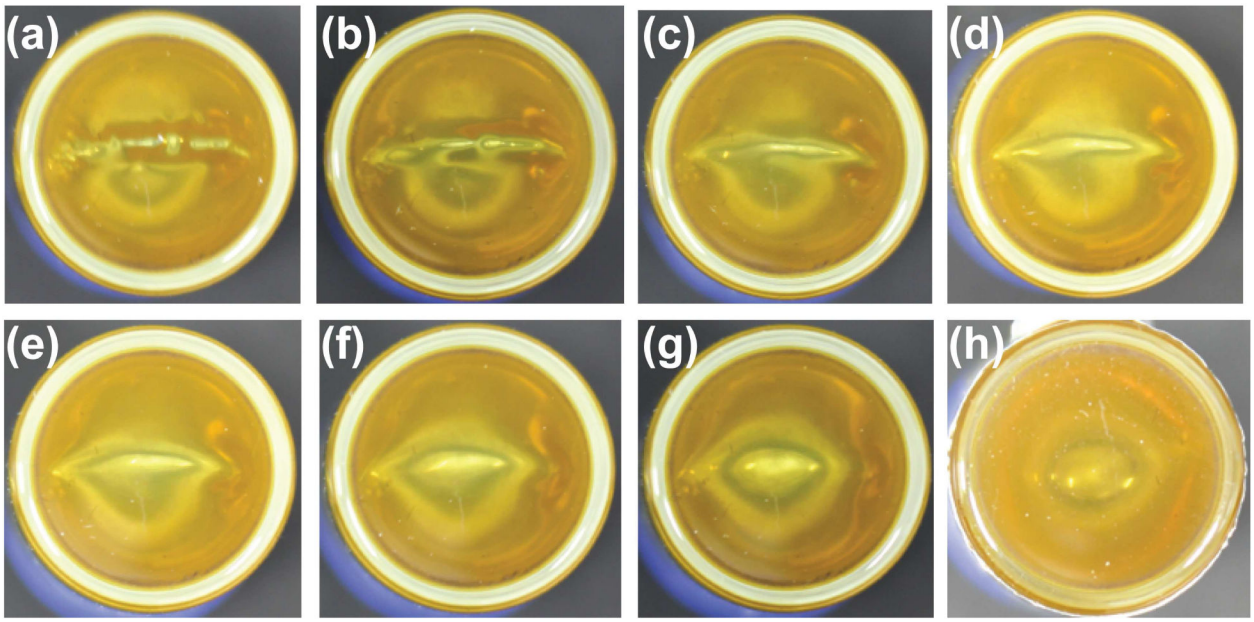

Figure 5.

Photographs of the self-healing process of the supramolecular gel **6**. The gel was cut and left standing for (a) 0 min; (b) 0.5 min; (c) 1.0 min; (d) 1.5 min; (e) 2.0 min; (f) 2.5 min; (g) 3.0 min and (h) 4.0 min.

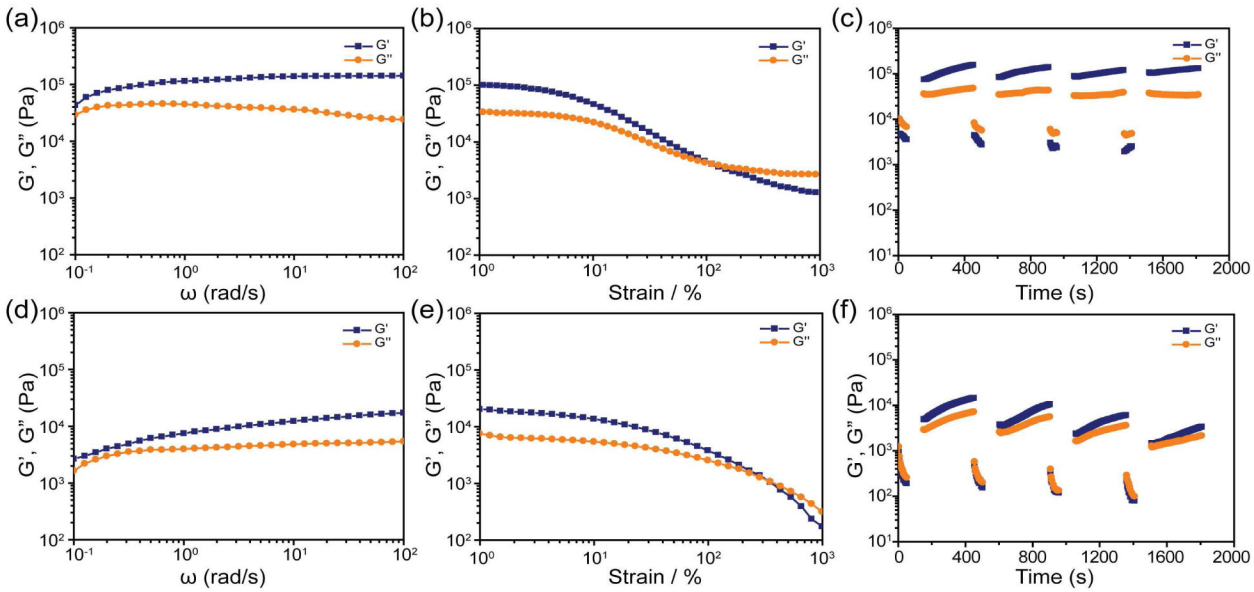

Figure 6.

Storage modulus (*G*') and loss modulus (*G*") values of gel **6**: (a) versus frequency (*ω*); (b) on strain sweep; (c) in continuous step strain measurements, gel **6** was subjected to 300% strain for 60 s, then go back to 0.1% strain in the linear regime for 300 s, and four cycles were done. Storage modulus (*G*') and loss modulus (*G*") values of gel **8**: (d) versus *ω*; (e) on strain sweep; (f) in continuous step strain measurements, gel **8** was subjected to 300% strain for 60 s, then go back to 0.1% strain in the linear regime for 300 s, and four cycles were done. The scanning frequency used above was 10 rad/s.

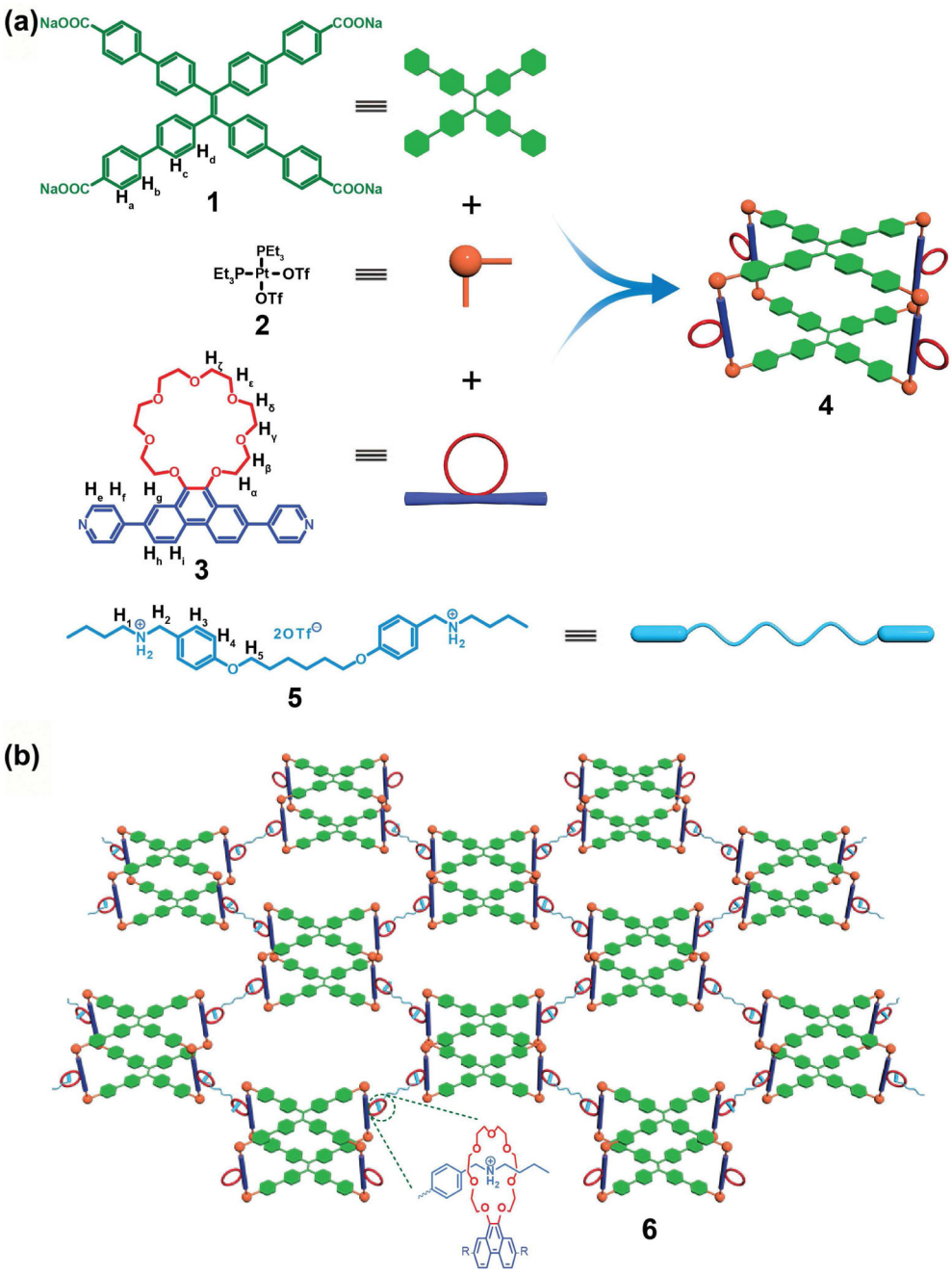

Scheme 1.

(a) Self-assembly of 21C7-functionalized metallacage **4** and (b) representation of the formation of a cross-linked SPN **6** from metallacage **4** and bisammonium salt **5**.

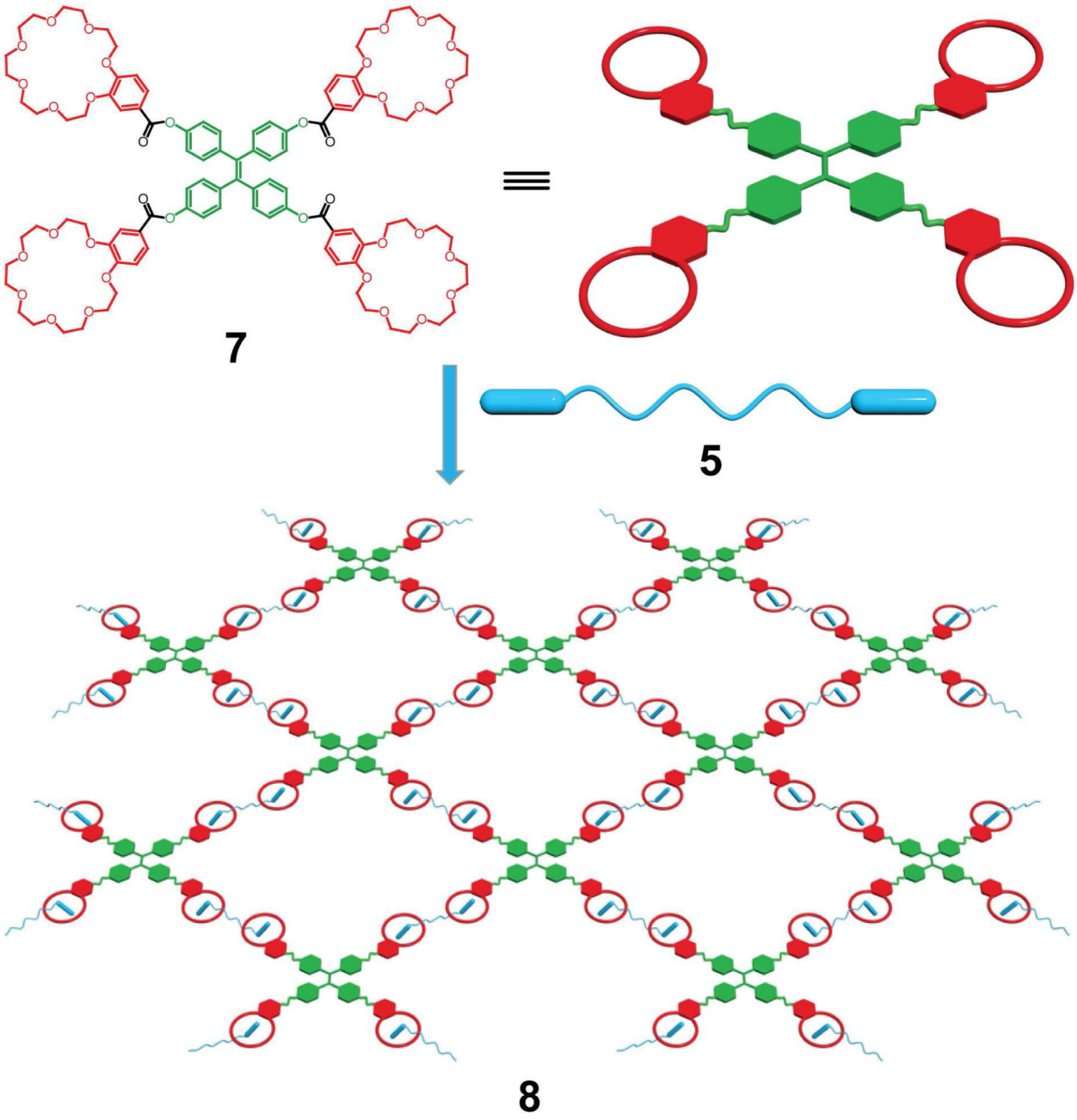

Scheme 2.

Representation of the formation of a cross-linked supramolecular polymeric network **8** from TPE-cored crown ether **7** and bisammonium salt **5**.